Spin-orbit stiffness of the spin-polarized electron gas

Florent Baboux, Florent Perez, C. A. Ullrich, G. Karczewski, T. Wojtowicz

Spin-orbit stiffness of the spin-polarized electron gas

F. Baboux,[1,2,*] F. Perez,[1,†] C. A. Ullrich,[3] G. Karczewski,[4] and T. Wojtowicz[4]

[1] *Institut des Nanosciences de Paris, CNRS/Université Paris VI, Paris 75005, France*
[2] *Laboratoire de Photonique et de Nanostructures (LPN), CNRS, Université Paris-Saclay, route de Nozay, 91460 Marcoussis, France*
[3] *Department of Physics and Astronomy, University of Missouri, Columbia, Missouri 65211, USA*
[4] *Institute of Physics, Polish Academy of Sciences, Warsaw, Poland*

In a spin-polarized electron gas, Coulomb interaction couples the spin and motion degrees of freedom to build propagating spin waves. The spin-wave stiffness $S_{\rm sw}$ quantifies the energy cost to trigger such excitation by perturbing the kinetic energy of the electron gas (i. e. putting it in motion). Here we introduce the concept of *spin-orbit stiffness*, $S_{\rm so}$, as the energy necessary to excite a spin wave with a spin polarization induced by spin-orbit coupling. This quantity governs the Coulombic enhancement of the spin-orbit field acting of the spin wave. First-principles calculations and electronic Raman scattering experiments carried out on a model spin-polarized electron gas, embedded in a CdMnTe quantum well, demonstrate that $S_{\rm so} = S_{\rm sw}$. Through optical gating of the structure, we demonstrate the reproducible tuning of $S_{\rm so}$ by a factor of 3, highlighting the great potential of spin-orbit control of spin waves in view of spintronics applications.

I. INTRODUCTION

Spintronics exploits the electronic spin degree of freedom to develop new functionalities for solid-state devices[1]. In this context, spin-orbit and Coulomb interactions have emerged as two protagonists. On the one hand, spin-orbit coupling, which transforms electric fields into effective magnetic fields, opens promising ways to manipulate the electronic spin through, e.g., spin orientation by electric current[3–5], spin Hall effect[6] or zero-bias spin separation[7]. On the other hand, Coulomb interactions govern the existence and behavior of spin waves[8,9], which can be used to transmit and modify logical information with reduced dissipation[10]. Both research paths can also usefully be combined: recently, the spin polarization generated by static[11] or oscillating[12] electric fields, through spin-orbit coupling, was used to trigger the precession of spin waves.

In the absence of spin-orbit effects, the spin-wave dispersion of an itinerant magnetic system can be written as $\hbar\omega_q = S_{\rm sw}\hbar^2 q^2/2m_b$, where $\mathbf{q}$ is the wavevector of the spin wave and m_b is the electron band mass[13]. $S_{\rm sw}$ is the *spin-wave stiffness*, which is the energy cost to excite an itinerant spin wave with a *kinetic* disturbance of the electrons[8]. The question then arises how the spin-wave dispersion is modified if spin-orbit coupling is present. In this paper, we will show that spin-orbit coupling adds a linear term to the spin-wave dispersion, which originates from the changes of the one-particle spin-orbit energies during a disturbance of the spin polarization. The related coefficient entering the spin-wave dispersion will be defined as the *spin-orbit stiffness* $S_{\rm so}$.

We have carried out a combined experimental and theoretical determination of the spin-wave and spin-orbit stiffnesses of a two-dimensional electron gas (2DEG). We find that $S_{\rm so} = S_{\rm sw}$: remarkably, the electron gas responds in the same manner to a kinetic or spin-orbit disturbance of its ground state. In addition, we show that $S_{\rm so}$ governs the Coulombic enhancement of the collective spin-orbit field $\mathbf{B}_{\rm SO}^{\rm coll}(\mathbf{q})$ acting on the spin-wave: $\mathbf{B}_{\rm SO}^{\rm coll}(\mathbf{q}) = S_{\rm so}\,\mathbf{B}_{\rm SO}(\mathbf{q})$, where $\mathbf{B}_{\rm SO}(\mathbf{q})$ is the single-particle spin-orbit field. We demonstrate the tuning of $S_{\rm so}$ by a factor of 3, by varying the electron density through optical gating[14,15]. From the point of view of potential applications such as spin-wave transistors[10,11], our results indicate that spin waves can be efficiently controlled via spin-orbit coupling, with the electron density as the tuning parameter.

II. THEORETICAL BACKGROUND

We consider the 2DEG embedded in a dilute magnetic CdMnTe quantum well[16–18]. In such system, the application of a moderate in-plane magnetic field (~ 1 T) polarizes the spins localized on the Mn impurities, which in turn polarizes the electron gas through exchange interaction[19]. This induces a giant Zeeman splitting Z (of order meV) of the electron gas, which dominates over the orbital quantization. One thus obtains a spin-polarized electron gas supporting spin wave excitations. The latter are collective precession of the itinerant spins, which were shown, theoretically[17] and experimentally[16,17,20,21], to obey the energy dispersion:

$$\hbar\omega_q = Z - \frac{1}{|\zeta|}\frac{Z}{Z^* - Z}\frac{\hbar^2}{2m_b}q^2\,, \qquad (1)$$

where ζ is the spin-polarization degree of the electron gas ($-1 \le \zeta \le 1$) and Z^* is Coulomb-renormalized Zeeman energy, i.e., the energy required to flip the spin of single electrons while keeping others unchanged[20]. Such spin-flip requires overcoming the Coulomb-exchange interaction between conduction electrons: thus, Z^* differs from Z by $2\partial\varepsilon_{\rm xc}/\partial\zeta$, where $\varepsilon_{\rm xc}$ is the exchange-correlation energy per particle of the electron gas[9]. In addition, ζ is also given by $-Z^*/2E_{\rm F}$ where $E_{\rm F}$ is the Fermi energy, such that the ratio Z^*/Z is linked to the spin-stiffness

ρ_s by $Z^*/Z = E_F/\rho_s$[9]. For a system with finite ζ, one obtains $\rho_s = \zeta^{-1}\partial\varepsilon/\partial\zeta$, with ε the *total* ground state energy per particle. Combined with the dispersion relation (1), this yields the spin-wave stiffness:

$$S_{sw} = \frac{1}{\zeta}\frac{\partial\varepsilon}{\partial\zeta}\left(\frac{\partial\varepsilon_{xc}}{\partial\zeta}\right)^{-1} . \quad (2)$$

Recently, the influence of spin-orbit coupling on the spin modes of 2DEGs, including the spin wave above, was investigated[18,22,23]. Due to internal electric fields arising from the inversion asymmetry of the confining potential (Rashba effect)[24] and of the crystalline cell (Dresselhaus effect)[25], spin-orbit coupling introduces an in-plane crystal magnetic field $\mathbf{B}_{SO}$ for each electron. To lowest order of the momentum $\mathbf{k}$, we have

$$\mathbf{B}_{SO}(\mathbf{k}) = 2\alpha\,(k_y, -k_x) + 2\beta\,(k_x, -k_y)\,, \quad (3)$$

with $\hat{x} \parallel [100]$ and $\hat{y} \parallel [010]$, and with α and β the single-particle Rashba and Dresselhaus coupling constants, respectively. These fields induce a distribution of spin splitting and spin orientation among electrons[26], which is a very efficient decoherence mechanisms in a macroscopic spin distribution[27]. However, Coulomb interaction breaks the expected scenario of such fast spin decoherence: the spin wave averages over the single-particle spin-orbit coupling and only experiences a macroscopic *collective* spin-orbit field $\mathbf{B}_{SO}^{coll}(\mathbf{q})$, which depends on the spin-wave momentum $\mathbf{q}$.

The field $\mathbf{B}_{SO}^{coll}(\mathbf{q})$ was found[18,23] to be proportional to the single-particle field $\mathbf{B}_{SO}(\mathbf{q})$ acting on individual electrons. As we will see below, the proportionality factor corresponds exactly to the spin-orbit stiffness introduced in the beginning:

$$\mathbf{B}_{SO}^{coll}(\mathbf{q}) = S_{so}\,\mathbf{B}_{SO}(\mathbf{q})\,. \quad (4)$$

It was shown that $S_{so} = 5.2$ for the GaAs quantum well of Ref.[23] and $S_{so} = 6.5$ for the CdMnTe quantum well of Ref.[18]. This already shows that the influence of spin-orbit fields on a spin wave is more complex than for a drifting spin packet, which simply precesses in the individual spin-orbit field $\mathbf{B}_{SO}(\mathbf{q}_{drift})$ felt by an electron with the drift momentum $\mathbf{q}_{drift}$[28–30].

The collective spin-orbit field $\mathbf{B}_{SO}^{coll}(\mathbf{q})$ can be superimposed with other magnetic fields[18,23]. In the present case of CdMnTe, it adds up to the giant Zeeman field coming from magnetic impurities, such that Eq. (1) becomes $\hbar\omega_q = |Z\mathbf{u} + \mathbf{B}_{SO}^{coll}(\mathbf{q})| - S_{sw}\hbar^2q^2/2m_b$, where $\mathbf{u} = \mathbf{B}_{ext}/B_{ext}$. This yields for the spin wave dispersion, in presence of spin-orbit coupling:

$$\hbar\omega_q \simeq Z - S_{sw}\frac{\hbar^2}{2m_b}q^2 - S_{so}(\alpha + \beta\sin 2\varphi)2q\,. \quad (5)$$

III. EXPERIMENTAL SIGNATURES OF SPIN-ORBIT COUPLING

Figure 1a illustrates the angle φ between the momentum $\mathbf{q}$ and the [100] axis, and also the orientation of $\mathbf{B}_{ext}$.

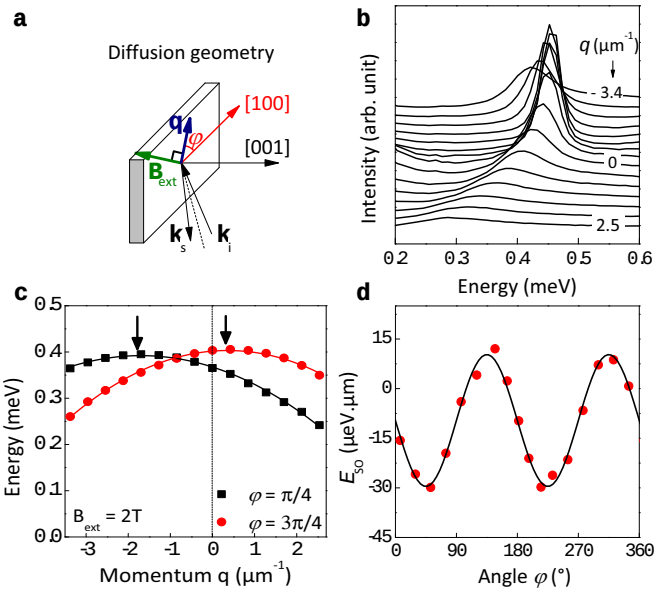

Figure 1. (a) Inelastic light scattering (ERS) geometry: $\boldsymbol{k}_i$ and $\boldsymbol{k}_s$ are the incoming and scattered light wavevectors, respectively; $\mathbf{q}$ is the transferred momentum, of in-plane orientation measured by the angle φ from [100]. An external magnetic field $\mathbf{B}_{ext}$ is applied perpendicular to $\mathbf{q}$. (b) ERS spectra of the spin wave, obtained at $B_{ext} = 2$ T and $\varphi = \pi/4$, for a series of transferred momenta q. (c) Wavevector dispersion of the spin wave for $\varphi = \pi/4$ and $\varphi = 3\pi/4$. (d) Variation of the linear term E_{SO} of the spin-wave dispersion (see text) as a function of the in-plane angle φ.

Figures 1b-d highlight the spin-orbit features of Eq. (5). To measure the spin-wave dispersion, we have employed electronic Raman scattering (ERS), which transfers a well-controlled momentum $\mathbf{q}$ to the spin excitations of the electron gas embedded in a quantum well[16,31]. We consider an asymmetrically modulation-doped, 20 nm-thick $Cd_{1-x}Mn_xTe$ ($x \simeq 0.13\%$) quantum well, grown along the [001] direction by molecular beam epitaxy, and immersed in a superfluid helium bath (2 K). The electronic density is $n_{2D} = 2.7\times10^{11}$ cm^{-2} and the mobility is 1.7×10^5 cm^{2}V^{-1}s^{-1}. Our setup, shown in Fig. 1a, allows us to vary $\mathbf{q}$ both in magnitude and in-plane orientation. The magnetic field $\mathbf{B}_{ext}$ is applied in the plane of the well, always perpendicular to $\mathbf{q}$. The incoming and scattered light are cross-polarized, so as to selectively probe spin excitations only[16].

Figure 1b displays a series of spin-wave ERS lines. They were obtained at fixed $B_{ext} = 2$ T and $\varphi = \pi/4$, but for transferred momenta q between -3.4 and $+2.5$ μm^{-1} (the positive sign is defined by the orientation of $\mathbf{q}$ in Fig. 1a). The corresponding wave-vector dispersion is plotted in Fig. 1c (squares): it shows a quadratic dependence with q, with a maximum shifted from the zone center. The dispersion for $\varphi = 3\pi/4$ (circles) has its maximum at a different value of q. These characteristics are consistent with Eq. (5) and are signatures of the spin-orbit contribution.

By fitting the dispersions to Eq. (5), we extract the spin-wave stiffness $S_{\rm sw}$ and the spin-orbit term $E_{\rm SO}(\varphi) = -2S_{\rm so}\,(\alpha + \beta \sin 2\varphi)$. We repeat the procedure for a series of in-plane angles φ, and plot $E_{\rm SO}(\varphi)$ in Fig. 1d. The experimental variation $E_{\rm SO}(\varphi)$ is in excellent agreement with the predicted sinusoidal variation. Using this procedure we obtain $S_{\rm sw} = 30.6 \pm 0.6$, and $S_{\rm so}\alpha = 46.7 \pm 1.2$ meV$\AA$, $S_{\rm so}\beta = 93.0 \pm 2.3$ meV$\AA$. The two latter quantities completely determine the collective spin-orbit field $\mathbf{B}_{\rm SO}^{\rm coll}(\mathbf{q})$ [Eq. (4)] acting of the spin wave: they define collective Rashba and Dresselhaus coupling constants, respectively, which are enhanced with respect to their single-particle counterparts by the spin-orbit stiffness $S_{\rm so}$.

IV. CALCULATION OF THE SPIN-ORBIT STIFFNESS

We have carried out a first-principles calculation of the spin-orbit stiffness $S_{\rm so}$. The calculation adapts the linear-response formalism developed earlier for the case of intersubband excitations[22,32,33] to calculate the spin-wave dispersions of a spin-polarized 2DEG in a quantum well with spin-orbit coupling. To first order in α and β and to second order in the wavevector $\mathbf{q}$, we obtain after a rather involved calculation the following, surprisingly simple analytic result for the spin-wave dispersion:

$$\hbar\omega_q = Z - S_{\rm sw}(\Delta\varepsilon_{\rm kin} + \Delta\varepsilon_{\rm so})\,. \qquad (6)$$

Here, $\Delta\varepsilon_{\rm kin} = \hbar^2 q^2/2m_b$ is the single-particle kinetic energy change and $\Delta\varepsilon_{\rm so} = \mathbf{B}_{\rm SO}(\mathbf{q})\cdot\mathbf{u} = (\alpha + \beta\sin 2\varphi)\,2q$ is the single-particle spin-energy change. Both contributions originate in the motion of electrons activated by the transfer of momentum $\mathbf{q}$. Comparing Eqs. (5) and (6), one immediately identifies the spin-orbit stiffness as

$$S_{\rm so} = S_{\rm sw}\,, \qquad (7)$$

which is the central theoretical result of this work. This equality means that, remarkably, the electron gas responds with the same stiffness to a kinetic or spin disturbance of its ground state.

V. VERIFICATION OF THE THEORY

To test the result of Eq. (7), we will explore the density dependence of the spin-wave and spin-orbit stiffnesses. For this we illuminate the quantum well with an above-barrier cw green laser beam (514.5 nm) to depopulate the electron gas[14,15]. By fitting the energy of the $q = 0$ spin wave versus $B_{\rm ext}$ with a Brillouin function [see Eq. (1) of Ref. 18], we checked that the green beam does not alter the temperature of the system by more than 0.3 K. We calibrate the density changes caused by the green illumination by extracting the Fermi energy $E_{\rm F}$ in two independent ways: from the width of the photoluminescence (PL) spectra, and from the slope of the cross-polarized ERS spectra of the single-particle excitations at zero spin polarization, as detailed in Ref.[34]. The corresponding values of $n_{\rm 2D}$ are plotted in Fig. 2a. Both determinations are in good agreement, showing that the electron density can be reproducibly tuned by a factor of 2 in our sample.

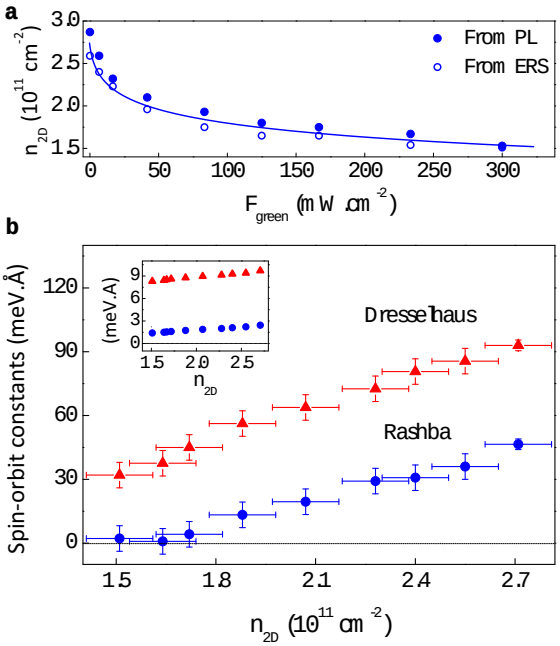

Figure 2. (a) Electron density as a function of the power density $F_{\rm green}$ of a secondary green laser beam, used to depopulate the electron gas. Density values are extracted from photoluminescence (solid circles) and ERS (empty circles) data. The line is a fit to the theory of Chaves *et al.*[14]. (b) Variation of the Rashba ($S_{\rm so}\alpha$, blue circles) and Dresselhaus ($S_{\rm so}\beta$, red triangles) collective coupling constants with the electron density. Inset: Calculated Rashba ($\alpha_{\rm kp}$, blue circles) and Dresselhaus ($\beta_{\rm kp}$, red triangles) single-particle coupling constants.

We can now determine how the changes in $n_{\rm 2D}$ affect the spin-wave and spin-orbit stiffnesses. For a series of electron densities, we extract at fixed $B_{\rm ext} = 2$ T, the quantities $S_{\rm sw}$, $S_{\rm so}\alpha$ and $S_{\rm so}\beta$ by fitting the dispersions to Eq. (5), as above. We first concentrate on the spin-wave stiffness, and plot in Fig. 3b the experimental $S_{\rm sw}$ (orange squares) as a function of $n_{\rm 2D}$. We compare it to the theory of Eq. (2) (solid orange line): for this we calculate $S_{\rm sw} = \frac{2E_{\rm F}}{Z^*-Z}\frac{Z}{Z^*}$, using the experimental Zeeman energy Z and Fermi energy $E_{\rm F}$, and calculating Z^* following Ref.[20]. An excellent agreement is found between theory and experiment. Next we consider the spin-orbit terms. Figure 2b shows the experimental $S_{\rm so}\alpha$ (blue circles) and $S_{\rm so}\beta$ (red triangles) as a function of $n_{\rm 2D}$. The Dresselhaus part $S_{\rm so}\beta$ exhibits a strong variation from 93 to 26 meV$\AA$, while the Rashba contribution $S_{\rm so}\alpha$ varies dramatically from 47 meV$\AA$ to nearly zero as the density is lowered.

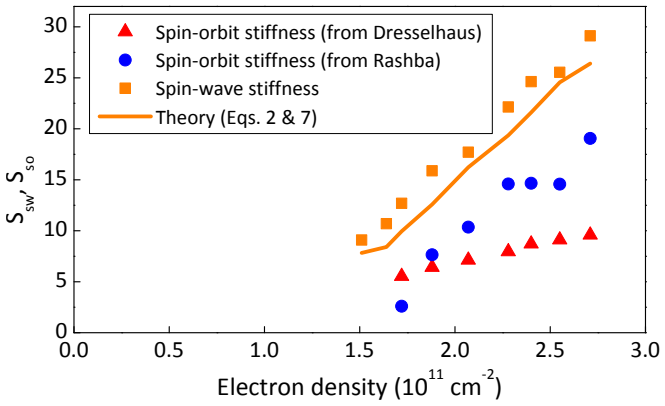

Figure 3. Spin-orbit stiffness ($S_{\rm so}$) and spin-wave stiffness ($S_{\rm sw}$) as a function of the electron density. Orange: spin-wave stiffness, as extracted experimentally from the curvature of the spin-wave dispersion (squares), and calculated using Eq. (2) (line). Blue circles: spin-orbit stiffness determined from the ratio $S_{\rm so}\alpha/\alpha_{\rm kp}$. Red triangles: spin-orbit stiffness determined from the ratio $S_{\rm so}\beta/\beta_{\rm kp}$.

Having determined the collective spin-orbit coupling constants $S_{\rm so}\alpha$ and $S_{\rm so}\beta$ for various electron densities, the remaining task to obtain $S_{\rm so}$ is to determine the single-particle spin-orbit constants α and β. To that end, we perform a self-consistent Schrödinger-Poisson calculation of the confining potential and electronic wavefunction. We then calculate the Rashba coefficient $\alpha_{\rm kp} = r_{41}^{6c6c} e\langle E_z\rangle$ and the Dresselhaus coefficient $\beta_{\rm kp} = \gamma\langle k_z^2\rangle$[26]. Here, r_{41}^{6c6c} and γ are material-dependent parameters, e is the electronic charge and E_z, k_z are respectively the electric field and wavevector along the growth axis. Using $r_{41}^{6c6c} = 6.93$ Å^2 and $\gamma = 43.9$ eVÅ^3 calculated by $\mathbf{k}\cdot\mathbf{p}$ perturbation theory[26] for CdTe, we show the calculated $\alpha_{\rm kp}$ and $\beta_{\rm kp}$ as a function of the electron density in the inset of Fig. 2b.

We can now plot in Fig. 3 the experimental spin-orbit stiffness $S_{\rm so}$, as given by $S_{\rm so}\alpha/\alpha_{\rm kp}$ (blue circles) and $S_{\rm so}\beta/\beta_{\rm kp}$ (red triangles). Both quantities slightly differ from each other and from the experimental spin-wave stiffness. It is difficult to discuss the relevance of this discrepancy, because α and β subtly depend on the exact shape of the wavefunction and confining potential, which are calculated here in a simple model. But despite these quantitative differences, we not that the qualitative increase of the spin-orbit stiffness with the density, as predicted by Eq. (7), is clearly attested experimentally. Figure 3 demonstrates that the experimental spin-orbit stiffness can be reproducibly tuned from 2-5 to 10-20, by changing the density by a factor of 2 only.

In conclusion, we have investigated the spin-orbit stiffness $S_{\rm so}$ of a model spin-polarized electron gas confined in a CdMnTe quantum well. From first-principles calculations we showed that $S_{\rm so} = S_{\rm sw}$, where $S_{\rm sw}$ is the spin-wave stiffness. This result means that the electron gas responds in the same manner to a kinetic or spin-orbit disturbance of its ground state. We further employed electronic Raman scattering on a diluted magnetic quantum well of CdMnTe, and used optical gating to study the density dependence of $S_{\rm so}$ and test our theory. We demonstrated the tuning of $S_{\rm so}$, which governs the magnitude of the spin-orbit field acting of the spin wave, by a factor of 3. In the perspective of a spin-wave based transistor[10,11], our findings thus suggest the ability to efficiently switch such transistor by tuning the spin-orbit stiffness through the electron density.

Acknowledgments: We thank Irene D'Amico for fruitful discussions and Mathieu Bernard & Silbé Majrab for technical support. F.B. and F.P. acknowledge support from the Fondation CFM, C'NANO IDF and ANR. C.A.U. is supported by DOE Grant No. DE-FG02-05ER46213. The research in Poland was partially supported by the National Science Centre (Poland) through Grants No. DEC-2012/06/A/ST3/00247 and No. DEC-2014/14/M/ST3/00484.

* florent.baboux@lpn.cnrs.fr
† florent.perez@insp.upmc.fr

1 I. Žutić, J. Fabian, and S. Das Sarma, Rev. Mod. Phys. **76**, 323 (2004).
2 M. I. D'yakonov and V. I. Perel', Phys. Lett. A **35**, 459 (1971).
3 S.D. Ganichev, S.N. Danilov, P. Schneider, V.V. Belkov, L.E. Golub, W. Wegscheider, D. Weiss and W. Prettl, Journal of Magnetism and Magnetic Materials **300**, 127 (2006).
4 Y. K. Kato, R. C. Myers, A. C. Gossard, and D. D. Awschalom, Phys. Rev. Lett. **93**, 176601 (2004).
5 A. Y. Silov, P. A. Blajnov, J. H. Wolter, R. Hey, K. H. Ploog and N. S. Averkiev Appl. Phys. Lett. **85**, 5929 (2004).
6 Y. K. Kato, R. C. Myers, A. C. Gossard, and D. D. Awschalom, Science **306**, 1910 (2004).
7 S. D. Ganichev, S. A. Tarasenko, V. V. Belkov, P. Olbrich, W. Eder, D. R. Yakovlev, V. Kolkovsky, W. Zaleszczyk, G. Karczewski, T. Wojtowicz, and D. Weiss, Phys. Rev. Lett. **102**, 156602 (2009).
8 D. Stancil and A. Prabhakar, Spin Waves (Springer, New York, 2009).
9 G. Giuliani and G. Vignale, Quantum theory of the electron liquid (Cambridge University Press, Cambridge, 2005).
10 V. V. Kruglyak, S. O. Demokritov, and D. Grundler, J. Phys. D: Appl. Phys. **43**, 264001 (2010).
11 Y. Kajiwara, K. Harii, S. Takahashi, J. Ohe, K. Uchida, M. Mizuguchi, H. Umezawa, H. Kawai, K. Ando, K. Takanashi, S. Maekawa, and E. Saitoh, Nature **464**, 262 (2010).
12 C. Ciccarelli, K. M. Hals, A. Irvine, V. Novak,

Y. Tserkovnyak, H. Kurebayashi, A. Brataas, and A. Ferguson, Nature Nanotech. **10**, 50 (2015).
[13] K. Yosida, Theory of Magnetism (Springer, Berlin, 1996).
[14] A. Chaves, A. Penna, J. Worlock, G. Weimann, and W. Schlapp, Surf. Sci. **170**, 618 (1986).
[15] D. Richards, G. Fasol, and K. Ploog, Appl. Phys. Lett. **57**, 1099 (1990).
[16] B. Jusserand, F. Perez, D. R. Richards, G. Karczewski, T. Wojtowicz, C. Testelin, D. Wolverson, and J. J. Davies, Phys. Rev. Lett. **91**, 086802 (2003).
[17] F. Perez, Phys. Rev. B **79**, 045306 (2009).
[18] F. Baboux, F. Perez, C. A. Ullrich, I. D'Amico, G. Karczewski, and T. Wojtowicz, Phys. Rev. B **87**, 121303(R) (2013).
[19] J. Gaj, R. Planel, and G. Fishman, Solid State Commun. **29**, 435 (1979).
[20] F. Perez, C. Aku-leh, D. Richards, B. Jusserand, L. C. Smith, D. Wolverson, and G. Karczewski, Phys. Rev. Lett. **99**, 026403 (2007).
[21] J. Gómez, F. Perez, E. M. Hankiewicz, B. Jusserand, G. Karczewski, and T. Wojtowicz, Phys. Rev. B **81**, 100403(R) (2010).
[22] C. A. Ullrich and M. E. Flatté, Phys. Rev. B **68**, 235310 (2003).
[23] F. Baboux, F. Perez, C. A. Ullrich, I. D'Amico, J. Gómez, and M. Bernard, Phys. Rev. Lett. **109**, 166401 (2012).
[24] Y. Bychkov and E. I. Rashba, J. Phys. C **17**, 6039 (1984).
[25] G. Dresselhaus, Phys. Rev. **100**, 580 (1955).
[26] R. Winkler, Spin-Orbit Coupling Effects in Two-Dimensional Electron and Hole Systems (Springer, Berlin, 2003).
[27] M. Dyakonov and V. Perel, Sov. Phys. Solid State **13**, 3023 (1972).
[28] V. Kalevich and V. Korenev, JETP Lett. **52**, 230 (1990).
[29] Y. K. Kato, R. C. Myers, A. C. Gossard, and D. D. Awschalom, Nature **427**, 50 (2004).
[30] L. Meier, G. Salis, I. Shorubalko, E. Gini, S. Schön, and K. Ensslin, Nature Phys. **3**, 650 (2007).
[31] A. Pinczuk, S. Schmitt-Rink, G. Danan, J. P. Valladares, L. N. Pfeiffer, and K. W. West, Phys. Rev. Lett. **63**, 1633 (1989).
[32] C. A. Ullrich and M. E. Flatté, Phys. Rev. B **66**, 205305 (2002).
[33] C. A. Ullrich, I. D'Amico, F. Baboux, and F. Perez, Proc. SPIE **8813**, 88132W (2013).
[34] C. Aku-Leh, F. Perez, B. Jusserand, D. Richards, W. Pacuski, P. Kossacki, M. Menant, and G. Karczewski, Phys. Rev. B **76**, 155416 (2007).